CO_2 Activation. 7.† Formation of the Catalytically Active Intermediate in the Hydrogenation of Carbon Dioxide to Formic Acid Using the [{(COD)Rh(μ-H)}$_4$]/ $Ph_2P(CH_2)_4PPh_2$ Catalyst: First Direct Observation of Hydride Migration from Rhodium to Coordinated 1,5-Cyclooctadiene

Franz Gassner, Eckhard Dinjus, Helmar Görls, and Walter Leitner*,‡

Arbeitsgruppe CO_2-Chemie der Max-Planck-Gesellschaft an der Friedrich-Schiller-Universität Jena, Lessingstrasse 12, 07743 Jena, FRG

Received November 27, 1995⊗

The nature of the catalytically active intermediate formed *in situ* from the tetrameric cluster [{(COD)Rh(μ-H)}$_4$] (COD = 1,5-cyclooctadiene; **1**) and the bidentate phosphane $Ph_2P(CH_2)_4PPh_2$ (dppb) during hydrogenation of CO_2 to formic acid was investigated. Kinetic measurements suggest the initial formation of a catalyst precursor that reacts with dihydrogen to give the actual active species. NMR spectroscopic investigations of the reaction of **1** with dppb in THF-d_8 reveal three phosphorus-containing products that were fully characterized by one- and two-dimensional techniques, including 2D-(^{31}P,^{1}H)-COLOC spectra. The tetrameric hydride cluster [{(dppb)Rh(μ-H)}$_4$] (**2**) and the double-phosphane-substituted monomeric rhodium hydride [(dppb)$_2$RhH] (**3**) are formed as byproducts in low yield. The (phosphane)rhodium η^3-cyclooctenyl complex [(dppb)Rh(η^3-C_8H_{13})] (**4**), arising *via* hydride transfer from rhodium to coordinated COD, is the major product, containing about 80% of the dppb. Complex **4** was isolated from the mixture of products, and its molecular structure was determined by X-ray crystal diffraction. Hydrogenolysis of the allyl moiety in the presence of excess dppb was shown to yield **3** presumably via the 14e species [(dppb)RhH]. The results are most consistent with the formation of **4** as the actual precursor for the active species [(dppb)RhH] in the rhodium-catalyzed hydrogenation of CO_2 to formic acid using *in situ* catalysts consisting of **1** and dppb.

Introduction

The hydrogenation of CO_2 to formic acid is a promising approach to the use of CO_2 as a raw material in chemical synthesis.[1,2] Late-transition-metal complexes act as homogeneous catalysts for this process, and efficient catalytic systems are known to operate in organic solvents,[3,4] in aqueous solutions,[5] and under supercritical conditions.[6] Experimental[3b,7] and theoretical[8] studies have shown that CO_2 insertion into the rhodium−hydride bond of the 14e species [(P_2)RhH] (P_2 = chelating bisphosphane) is most likely the key step during the catalytic cycle of CO_2 hydrogenation in dipolar nonprotic solvents under the conditions summarized in eq 1. The 14e species [(P_2)RhH] tend to form

$$H_2 + CO_2 \xrightarrow[T = 25\ ^\circ C,\ p_0 = 40\ atm]{solvent,\ NEt_3} HCO_2H \qquad (1)$$

oligomers of type [{(P_2)Rh(μ-H)}$_x$], and the catalytic behavior of these clusters in hydrogenation reactions has been studied in detail, namely by the groups of Muetterties[9] and Fryzuk.[10]

We have recently reported on the use of the tetrameric rhodium hydride cluster [{(COD)Rh(μ-H)}$_4$] (COD = 1,5-cyclooctadiene; **1**) in the presence of the chelating phosphane $Ph_2P(CH_2)_4PPh_2$ (dppb) as a very efficient homogeneous catalyst for the hydrogenation of CO_2 to

† Part 6: Reference 3d.

‡ Current address: Max-Planck-Institut für Kohlenforschung, Kaiser-Wilhelm-Platz 1, 45470 Mülheim/Ruhr, FRG; Fax: +49-208-306 2980. E-mail: leitner@mpi-muelheim.mpg.de.

⊗ Abstract published in *Advance ACS Abstracts,* March 15, 1996.

(1) (a) Behr, A. *Carbon Dioxide Activation by Metal Complexes*; VCH: Weinheim, Germany, 1988. (b) Ayers, W. M., ed. *Catalytic Activation of Carbon Dioxide*; ACS Symposium Series 363; American Chemical Society: Washington, DC, 1988. (c) Aresta, M.; Schloss, J. V., Eds. *Enzymatic and Model Carboxylation and Reduction Reactions for Carbon Dioxide Utilization*; NATO ASI Series C, No. 314; Kluwer Academic Press: Dordrecht, The Netherlands, 1990.

(2) (a) Jessop, P. G.; Ikariya, T.; Noyori, R. *Chem. Rev.* **1995**, *95*, 259. (b) Leitner, W. *Angew. Chem.* **1995**, *107*, 2391; *Angew. Chem., Int. Ed. Engl.* **1995**, *34*, 2207. (c) Leitner, W. *Coord. Chem. Rev.*, in press.

(3) (a) Graf, E.; Leitner, W. *J. Chem. Soc., Chem. Commun.* **1992**, 623. (b) Leitner, W.; Dinjus, E.; Gassner, F. *J. Organomet. Chem.* **1994**, *475*, 257. (c) Fornika, R.; Görls, H.; Seemann, B.; Leitner, W. *J. Chem. Soc., Chem. Commun.* **1995**, 1479. (d) Graf, E.; Leitner, W. *Chem. Ber.* **1996**, *129*, 91.

(4) (a) Inoue, Y.; Izumida, H.; Sasaki, Y.; Hashimoto, H. *Chem. Lett.* **1976**, 863. (b) Tsai, J.-C.; Nicholas, K. M. *J. Am. Chem. Soc.* **1992**, *114*, 5117. (c) Lau, C. P.; Chen, Y. Z. *J. Mol. Catal. A: Chem.* **1995**, *101*, 33.

(5) (a) Taqui Khan, M. M.; Halligudi, S. B.; Shukla, S. *J. Mol. Catal.* **1989**, *57*, 47. (b) Gassner, F.; Leitner, W. *J. Chem. Soc., Chem. Commun.* **1993**, 1465.

(6) a) Jessop, P. G.; Ikariya, T.; Noyori, R. *Nature* **1994**, *368*, 231. (b) Jessop, P. G.; Ikariya, T.; Noyori, R. *Science* **1995**, *269*, 1065. (c) Jessop, P. G.; Hsiao, Y.; Ikariya, T.; Noyori, R. *J. Am. Chem. Soc.* **1996**, *118*, 344.

(7) Burgemeister, T.; Kastner, F.; Leitner, W. *Angew. Chem.* **1993**, *105*, 781; *Angew. Chem., Int. Ed. Engl.* **1993**, *32*, 739.

(8) Hutschka, F.; Dedieu, A.; Leitner, W. *Angew. Chem.* **1995**, *107*, 1905; *Angew. Chem., Int. Ed. Engl.* **1995**, *34*, 1742.

(9) (a) Day, V. W.; Fredrich, M. F.; Reddy, G. S.; Sivak, A. J.; Pretzer, W. R.; Muetterties, E. L. *J. Am. Chem. Soc.* **1977**, *99*, 8091. (b) Sivak, A. J.; Muetterties, E. L. *J. Am. Soc. Chem.* **1979**, *101*, 4878.

(10) (a) Fryzuk, M. D. *Can. J. Chem.* **1983**, *61*, 1347. (b) Fryzuk, M. D.; Piers, W. E.; Einstein, F. W. B.; Jones, T. *Can. J. Chem.* **1989**, *67*, 883.

0276-7333/96/2315-2078$12.00/0

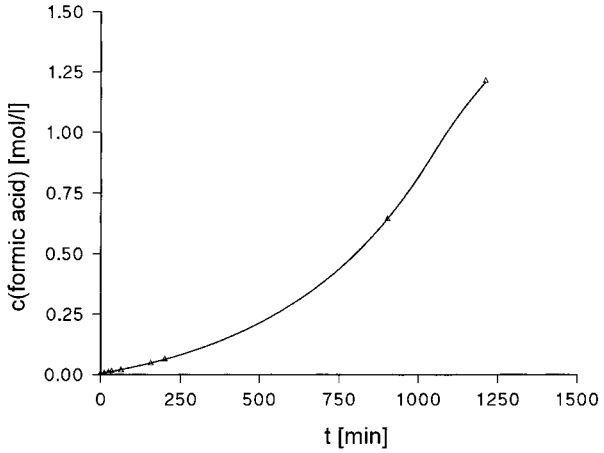

Figure 1. Catalytic formation of formic acid by hydrogenation of CO_2 in acetone/NEt_3 solution using the *in situ* catalyst **1**/dppb. Reaction conditions: solvents acetone/NEt_3 (5:1); $c(Rh) = 2.47 \times 10^{-3}$ mol L^{-1}; dppb/Rh = 1.2; room temperature; $p_0 = 40$ atm.

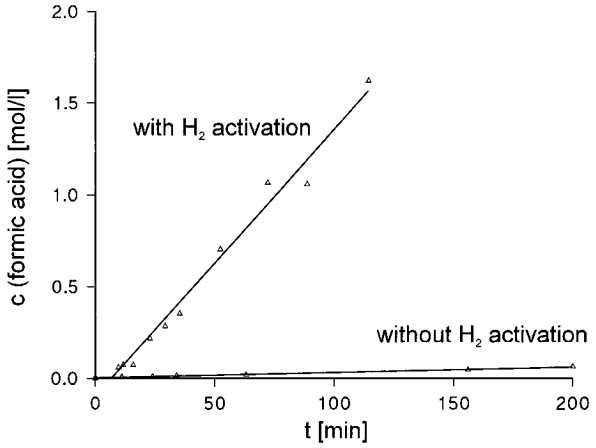

Figure 2. Activation of the in situ catalyst **1**/dppb in acetone/NEt_3 by pre-hydrogenation. For reaction conditions, see Figure 1.

formic acid under the conditions summarized in eq 1.[3b] One possible explanation for the much higher activity of the hydride-bridged precursor **1** compared to that of its chloride analog [{(COD)Rh(μ-Cl)}$_2$] is the direct formation of the catalytically active 14e species [(dppb)-RhH] or its oligomers [{(dppb)Rh(μ-H)}$_x$] by COD substitution from **1**.[3b] However, derivatives of the species [{(P_2)Rh(μ-H)}$_x$] containing dppb or other bidentate phosphanes bearing aryl groups at phosphorus have not been described up to now. Furthermore, no information was available on the reactivity of **1** toward phosphanes. We therefore decided to investigate the pathway of formation of the actual catalytically active species from the *in situ* catalyst consisting of **1** and dppb in more detail.

Results and Discussion

One criterion for the direct formation of a catalytically active species from *in situ* catalysts is the absence of an induction period; i.e., catalysis must start immediately with the maximum turnover frequency as soon as the reactants are introduced. The kinetics of the catalytic hydrogenation of CO_2 to formic acid in dipolar aprotic solvent systems can be followed readily by NMR spectroscopy.[3a–c] Acetone has been suggested as the preferred solvent for this type of experiment, as it yields homogeneous reaction solutions in the presence of trialkylamines under all conditions.[3b] Figure 1 shows the catalytic formation of formic acid when a solution of **1** (2.5 mmol L^{-1} in rhodium) and dppb (3.0 mmol L^{-1}) in a 5:1 mixture of acetone and triethylamine is stirred under a roughly equimolar atmosphere of CO_2 and H_2 at a total pressure of 40 atm at room temperature. The initial rate of formic acid formation is very slow (turnover frequency (tof) = 7.2 h^{-1}) but increases during the course of reaction. After 20 h, the equilibrium concentration of formic acid under the given conditions (1.75 mol L^{-1} [3b]) is not yet reached and a total of 480 catalytic cycles are performed during this period of time. A maximum turnover frequency of 44 h^{-1} is obtained from the slope of the concentration profile shown in Figure 1. These results are surprising in view of the excellent performance of the same catalyst in batch reactions using the DMSO/NEt_3 solvent system. Turnover numbers up to 2200 have been reported, and a lower limit for the turnover frequency of 375 h^{-1} has been estimated in this case.[3b]

Similar to other rhodium catalysts,[3b,4b] the *in situ* system **1**/dppb can be activated by treatment with dihydrogen *prior* to reaction, as illustrated in Figure 2. After pre-hydrogenation of the acetone/NEt_3 solution containing **1** and dppb with 20 atm of H_2 for 1 h, catalysis starts immediately with a maximum turnover frequency of 354 h^{-1}, i.e. 50 times faster than without pre-hydrogenation under otherwise identical conditions. These findings lead to the conclusion that—at least in acetone/NEt_3—the catalytically active species for CO_2 hydrogenation is *not formed directly* from **1** and dppb under catalytic conditions.

Further information on the formation of the active species comes from stoichiometric reactions of **1** and dppb as investigated by NMR spectroscopy. THF-d_8 was used as a solvent in these experiments for solubility reasons. The characteristic high-field ^1H NMR signal (δ −12.05, qt, $^1J_{RhH}$ = 14.2 Hz) for the hydride **1**[11] disappears immediately when 4 equiv of dppb (1 equiv per rhodium atom) is added as a solid in one portion to a THF-d_8 solution of **1** at room temperature. The ^{31}P NMR spectrum shows three new sets of signals indicating the formation of (phosphane)rhodium complexes. The main product exhibits a doublet at δ 38.2 with a coupling constant $^1J_{RhP}$ of 199.5 Hz. The second complex is characterized by a doublet at δ 27.0 with $^1J_{RhH}$ = 149 Hz. A third, very weak signal consists of a doublet of badly resolved multiplets centered at δ 35.5. The distance of the two multiplets corresponds to a $^1J_{RhP}$ coupling constant of 169 Hz. At the same time, two new signals in the high-field region of the ^1H NMR spectrum of the reaction mixture indicate the formation of rhodium hydride complexes. A quintet of doublets is centered at δ −11.2, and a multiplet consisting of at least seven lines appears at δ −11.8 ppm. Corresponding cross-peaks in the 2D-{^{31}P,^1H}-COLOC spectrum unequivocally demonstrate that these hydride signals arise from the same compound as the phosphorus signals at 27.0 and 35.5 ppm, respectively.

The ^{31}P broad-band-decoupled $^1H\{^{31}P\}$ NMR spectrum gives further evidence for the characterization of

(11) Kulzick, M.; Price, R. T.; Muetterties, E. L.; Day, V. W. *Organometallics* **1982**, *1*, 1256.

Scheme 1. Phosphorus-Containing Products from the Reaction of [{(COD)Rh(μ-H)}$_4$] (1) with dppb[a]

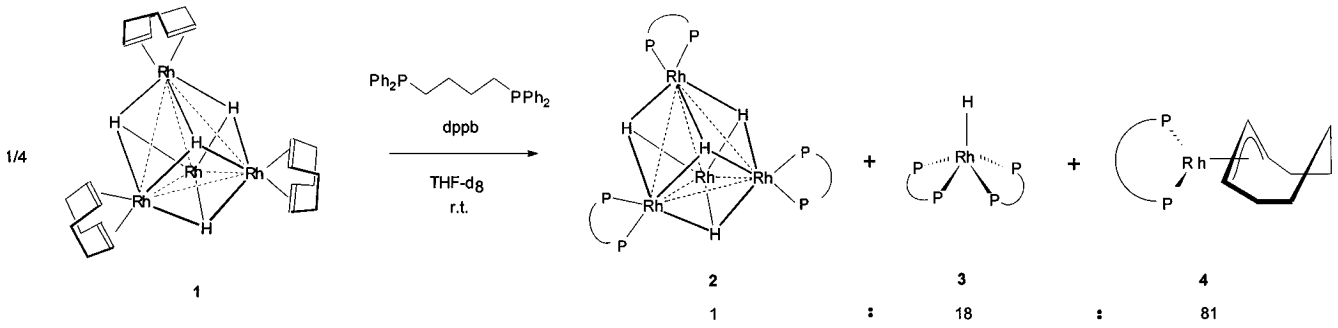

[a] The ratios were obtained from ^{31}P NMR spectra of the crude reaction mixture. No other phosphorus-containing compounds were detectable.[14]

the two hydride complexes. The signal at δ −11.2 ppm collapses to a doublet under these conditions, indicating that the original quintet structure arises from coupling with four equivalent P atoms. In agreement with NMR data for the known complexes [(P$_2$)$_2$RhH],[12b] we assign these signals to [(dppb)$_2$RhH] (**3**). It is noteworthy in this context that **3** is not accessible by common routes used for the synthesis of complexes [(P$_2$)$_2$RhH].[12] Our results show that this is due to limitations of these synthetic methodologies rather than the instability of **3**.

The formula [{(dppb)Rh(μ-H)}$_4$] (**2**) can be assigned to the second hydride-containing complex on the basis of its NMR data. The hydride signal of **2** appears as a quintet under ^{31}P-decoupled conditions, and this pattern is only explained if formation of a tetrameric cluster with fluxional hydrides similar to **1** is assumed.[11] The multiplet structure observed in the ^{31}P{^{1}H} NMR of this compound may arise from the higher order spin system formed by chemically equivalent, but magnetically inequivalent, ^{31}P and ^{103}Rh nuclei. Similar spectroscopic properties were reported for a tetrameric hydride-bridged cluster bearing a chelating phosphite ligand.[9a]

The major product of the reaction of **1** with dppb contains no hydride ligand, as is obvious from the absence of any cross-peak in the 2D-(^{31}P,^{1}H)-COLOC spectrum. A characteristic set of proton resonances consisting of a slightly broadened triplet at δ 5.30 and a quartet at δ 3.71 suggests the formation of the η^3-cyclooctenyl complex [(dppb)Rh(η^3-C$_8$H$_{13}$)] (**4**).[13] This assignment was confirmed by the 2D-(^{1}H,^{1}H)-COSY spectrum and ^{13}C-DEPT and 2D-(^{13}C,^{1}H)-HETCOR experiments. Scheme 1 summarizes the product distribution of the reaction of [{(COD)Rh(μ-H)}$_4$] (**1**) with dppb as revealed by NMR spectroscopy.[14]

The X-ray crystal structure analysis of complex **4** verified the NMR spectroscopic assignments (see Experimental Section for details). Crystals suitable for X-ray diffraction analysis of the pentane solvate **4**·0.5C$_5$H$_{12}$ were obtained by slow crystallization from light petroleum ether (bp 40−60 °C). The molecular structure of **4** together with some characteristic distances and angles is shown in Figure 3.

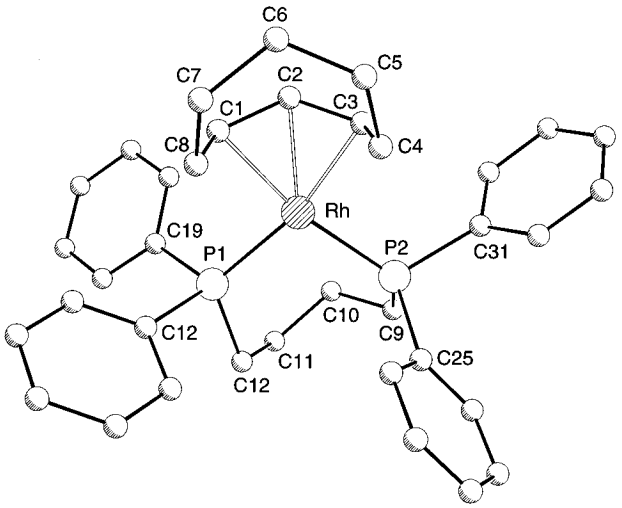

Figure 3. Molecular structure of [(dppb)Rh(η^3-C$_8$H$_{13}$)] (**4**) as determined by X-ray diffraction of **4**·0.5C$_5$H$_{12}$. Hydrogens were omitted for clarity. Selected distances (Å) and angles (deg): Rh−C1, 2.219(10); Rh−C2, 2.122(10); Rh−C3, 2.209(10); Rh−P1, 2.237(3); Rh−P2, 2.228(3); C1−C2, 1.409(14); C2−C3, 1.424(14); C3−C4, 1.491(14); C4−C5, 1.54(2); C5−C6, 1.51(2); C1−Rh−C3, 68.8(4); P1−Rh−P2, 98.63(10); C2−C1−C3, 124.0(10); [P1−Rh−P2]/[C1−Rh−C3], 6.0; [P1−Rh−P2]/[C1−C2−C3], 113.1.

The rhodium center in complex **4** is symmetrically bound to the two phosphorus atoms of the dppb ligand. The Rh−P distances and the P−Rh−P angle are in the typical range for rhodium dppb complexes.[3c,15] The seven-membered chelate ring has a twisted-boat conformation. The four atoms P1, P2, C1, and C3 form a nearly ideal square-planar arrangement around the rhodium center, the angle between P1−Rh−P2 and C1−Rh−C3 being 6°. The η^3-cyclooctenyl ligand adopts the expected[16] boatlike conformation and is symmetrically bound to the rhodium atom *via* the three allylic carbon atoms C1, C2, and C3. The hydrogen atoms on these allylic carbons and on the adjacent carbons C4−C8 are among those located on the difference map and do not exhibit any interaction with the rhodium center. The angle between the plane P1−Rh−P2 and the plane formed by the allylic carbon atoms is 113.1°. Nearly the same value is found for a bis(triphenylphosphane)-

(12) (a) Sacco, A.; Ugo, R. *J. Chem. Soc.* **1964**, 3274. (b) James, B. R.; Mahajan, D. *Can. J. Chem.* **1979**, *57*, 180.

(13) Fornika, R.; Dinjus, E.; Görls, H.; Leitner, W. *J. Organomet. Chem.* **1996**, *511*, 145.

(14) The formation of the bisphosphane complex **3** together with the stoichiometry of the reaction requires the presence of phosphane-free rhodium species. The presence of weak multiplets between 5.6 and 5.4 ppm in the ^{1}H spectrum indeed indicates the presence of such species, together with some free cyclooctene. The low concentration of these compounds together with severe overlap of signals in other parts of the proton spectrum did not allow a final assignment, however.

(15) Anderson, P. M.; Pignolet, L. H. *Inorg. Chem.* **1981**, *20*, 4101.

(16) (a) Jonas, K. *Angew. Chem.* **1985**, *97*, 292. (b) Braunstein, P.; Faure, T.; Knorr, M.; Strählfeldt, T.; DeCian, A.; Fischer, A. *Gazz. Chim. Ital.* **1995**, *125*, 35 and references therein.

rhodium complex containing the cyclooctadienyl ligand C_8H_{11}.[17]

In order to obtain further insight into the formation of **2**−**4**, complex **1** was reacted subsequently with 4 equiv of dppb *per* cluster unit. All three complexes **2**−**4** are formed in a constant ratio from the beginning, with the remaining cluster **1** staying intact. If a 2-fold excess of dppb *per* rhodium is employed, the three complexes are formed again and free dppb is observed in the $^{31}P\{^1H\}$ NMR spectrum. These results suggest that the reaction of **1** with dppb leads to the COD substitution product **2** only *via* a minor reaction pathway. Cleavage of the tetrameric core of **1** predominates, resulting in formation of the bisphosphane hydride complex **3** and the cyclooctenyl complex **4**, presumably *via* the common intermediate [(dppb)Rh(H)(COD)] (**5**). Formation of **3** and **4** *via* **2** can be excluded, as **2** has been found to be present in reaction mixtures containing free COD and dppb. The low reactivity of tetrameric clusters [{(P_2)-Rh(μ-H)}$_4$] toward excess P_2 has been noted also by Fryzuk et al.[10a] A similar pathway has been suggested most recently for the formation of cyclooctenyl complexes of rhodium by hydride transfer from formate to coordinated COD.[13]

Similarly to the tetrameric cluster, the cyclooctenyl complex **4** was found to be stable in the presence of excess dppb.[18] However, both compounds are readily converted to complex **3** when the reaction mixture is pressurized with 10 atm of dihydrogen in a high-pressure NMR tube. In the case of complex **4**, this reaction most likely involves removal of the η^3-allyl moiety by hydrogenolysis[10] whereafter the resulting 14e species [(dppb)RhH] is trapped immediately by excess dppb to yield **3** (eq 2).

$$\underset{\mathbf{4}}{[(\text{dppb})\text{Rh}(\eta^3\text{-}C_8H_{13})]} \xrightarrow[\text{THF-}d_8\text{, room temp}]{\text{10 atm of } H_2} \text{"[(dppb)RhH]"} \xrightarrow{\text{dppb}} \underset{\mathbf{3}}{[(\text{dppb})_2\text{RhH}]} \quad (2)$$

The possible formation of **4** under catalytic conditions was verified experimentally when **1** was reacted with dppb in a two-layer mixture resulting from addition of a solution of dppb in DMSO to a solution of **1** in NEt_3. The complexes **1** and **4** are contained exclusively in the NEt_3 layer under these conditions, but the system is known to be homogenized under catalytic conditions.[3b] As in THF-d_8, hydrogenolysis of **4** may then lead rapidly to the 14e species [(dppb)RhH] either stabilized as amine adduct[19] or as oligomer **2**.

Similarly, the initial formation of **4** readily explains the marked induction period for CO_2 hydrogenation using the **1**/dppb catalyst in acetone/NEt_3. In contrast to the situation in DMSO/NEt_3, hydrogenolysis of **4** appears to be sluggish in the presence of CO_2 in this case; the reason for this discrepancy is not yet clear. However, pre-hydrogenation of the catalyst solution with 20 atm of H_2 for 1 h cleanly leads to the catalytically active species, as shown by the high turnover frequency of 354 h^{-1}, which corresponds well to the lower limit of 375 h^{-1} estimated for the same catalyst in DMSO solution.

Conclusion

In conclusion, we have shown that the η^3-cyclooctenyl complex [(dppb)Rh(η^3-C_8H_{13})] (**4**) is formed as the major product in the reaction of the hydride cluster **1** and the chelating phosphane dppb. The molecular structure of **4** was elucidated by an X-ray crystal structure analysis, and direct transfer of hydride from rhodium to coordinated COD was demonstrated to account most likely for the formation of **4**. The η^3-cyclooctenyl ligand from **4** can be removed by reaction with dihydrogen leading to the 14e species [(dppb)RhH] that was trapped as the stable 18e rhodium hydride complex [$(dppb)_2$RhH] (**3**) in the presence of excess dppb.

The present findings imply that complex **4** is the actual catalyst precursor during CO_2 hydrogenation to formic acid using the *in situ* catalyst **1**/dppb. The results obtained from catalytic experiments under various conditions are in agreement with the initial formation of **4** and its hydrogenolysis to yield the 14e species [(dppb)RhH] that serves as the catalytically active species.

Experimental Section

General Comments. All manipulations were carried out under an atmosphere of argon using standard Schlenk techniques. The complex [{(COD)Rh(μ-H)}$_4$] (**1**) was synthesized according to a recently published procedure.[20] The phosphane dppb was obtained from Strem Chemicals and used without further purification. The high-pressure reactor used for catalytic experiments is described in detail elsewhere.[3b] NMR spectra were recorded on a Bruker AC 200F, operating at 200.13 MHz (^1H), 50.26 MHz (^{13}C), and 80.96 MHz (^{31}P). Broad-band ^{31}P decoupling was achieved using an external BSV 3BX decoupling unit. Chemical shifts are referenced to $SiMe_4$ using the solvent resonances as internal standards for ^1H and ^{13}C and to H_3PO_4 as external standard for ^{31}P. The 2D-$\{^1H,^{31}P\}$-COLOC spectra were carried out using standard Bruker software based on the pulse sequence reported in ref 21. The mixing time was optimized for a P−H coupling constant of ~10 Hz, as $^2J_{PH}$ is commonly between 5 and 20 Hz in (phosphane)rhodium hydride complexes.

Reaction of [{(μ-H)Rh(COD)}$_4$] (1) with dppb in THF-d_8. A solution of **1** (11.1 mg, 13.1 μmol) in 0.45 mL of THF-d_8 was placed in an NMR tube, and the phosphane dppb (22.3 mg, 52.2 μmol) was added as a solid in one portion or in four equal portions. The mixture was agitated until a clear homogeneous solution was obtained, and ^1H and $^{31}P\{^1H\}$ NMR spectra were recorded immediately after each addition. Characteristic spectroscopic data are as follows.

[{(dppb)Rh(μ-H)}$_4$] (**2**): ^1H NMR δ −11.8 (m, $^1J_{RhH}$ = 13.1 Hz, Rh−*H*); $^{31}P\{^1H\}$ NMR δ 35.5 (dm, $^1J_{RhP}$ = 169 Hz, Rh−*P*).

[$(dppb)_2$RhH] (**3**): ^1H NMR δ −11.2 (dqt, $^1J_{RhH}$ = 7.5 Hz, $^2J_{PH}$ = 19.9 Hz, Rh−*H*); $^{31}P\{^1H\}$ NMR δ 27.0 (d, $^1J_{RhP}$ = 146 Hz, Rh−*P*).

[(dppb)Rh(η^3-cyclooctenyl)] (**4**): ^1H NMR δ 5.30 (t, br, $^3J_{HH}$ = 7.9 Hz, ^1H, ≈C*H*≈), 3.71 (q, br, $^3J_{HH}$ = 7.9 Hz, 2H, =C*H*−); $^{31}P\{^1H\}$ NMR 38.2, d, $^1J_{RhP}$ = 199 Hz.

(17) Vitulli, G.; Raffaelli, A.; Costantino, P. A.; Barberini, C.; Marchetti, F.; Merlino, S.; Skell, P. S. *J. Chem. Soc., Chem. Commun.* **1983**, 232.

(18) Note that the related complex [(dppp)Rh(η^3-C_8H_{13})] reacts with excess dppp to give [$(dppp)_2$RhH] and 1,3-cyclooctadiene: Fornika, R. Ph.D. Thesis, Jena, Germany, 1994.

(19) Hofmann, P.; Meier, C.; Englert, U.; Schmidt, M. U. *Chem. Ber.* **1992**, *125*, 353.

(20) Bönnemann, H.; Brijoux, W.; Brinkmann, R.; Dinjus, E.; Fretzen, R.; Joussen, T.; Korall, B. *J. Mol. Catal.* **1992**, *74*, 323.

(21) Kessler, H.; Griesinger, C.; Zarbock, J.; Loosli, H. R. *J. Magn. Reson.* **1984**, *57*, 331.

Reaction of [{(μ-H)Rh(COD)}$_4$] (1) with Excess dppb and Dihydrogen in THF-d_8. **1** (7.3 mg, 8.6 μmol) was dissolved in 0.30 mL of THF-d_8, and dppb (29.3 mg, 68.7 μmol) was added as a solid in one portion. The solution was transferred to a thick-walled NMR tube (Wilmad 522-PV) by syringe, and ^{1}H and ^{31}P{^{1}H} NMR spectra were recorded. The tube was then pressurized to 10 atm with H_2 and carefully agitated, and spectra were recorded again. ***Caution!*** Handling of glass apparatus under high pressure is hazardous and has to be carried out under appropriate safety conditions.

Reaction of [{(μ-H)Rh(COD)}$_4$] (1) with dppb in a DMSO/NEt$_3$ Two-Phase System. A solution of dppb (29.1 mg, 68.3 μmol) in 15 mL of DMSO was layered with a solution of **1** (14.5 mg, 17.1 μmol) in 3.0 mL of NEt_3. After 15 h, samples were withdrawn from each layer and analyzed by ^{31}P-{^{1}H} NMR spectroscopy (unlocked). Complex **4** was identified as the only phosphorus-containing species in the NEt_3 phase, whereas only free dppb could be detected in the DMSO layer (δ −15.2, s).

Reaction of [{(μ-H)Rh(COD)}$_4$] (1) with dppb in THF and Isolation of [(dppb)Rh(η^3-C$_8$H$_{13}$)]·0.5C$_5$H$_{12}$ (4·0.5C$_5$H$_{12}$). **1** (72.8 mg, 85.8 μmol) was dissolved in 5 mL of THF; a solution of dppb (0.16 g, 0.38 mmol) in 5 mL THF was added at room temperature, and the mixture was stirred for 20 min. The solvent was removed and the residue thoroughly dried under high vacuum. The remaining solid was dissolved in a minimum of light petroleum ether (bp 40−60 °C), and the solution was placed in a refrigerator at −35 °C. The yellow crystals formed after 4 weeks were removed from the solvent and analyzed by NMR, mass spectroscopy, and X-ray crystal diffraction. Yield: 73.0 mg (0.10 mmol, 29%). Mp: 231 °C dec. EI-MS: *m*/*z* 638 (**4**$^+$), 529 (**4**$^+$ − C_8H_{13}), 425 (**4**$^+$ − C_8H_{13} − C_6H_5). ^{1}H NMR (C_6D_6): δ 7.8−7.4 (m, 8H, PPh, *m-H*), 7.3−6.7 (m, 12H, PPh, *o,p-H*), 5.27 (t, $^3J_{HH}$ = 7.9 Hz, 1H, ≈C*H*≈), 3.65 (q, $^3J_{HH}$ = 7.9 Hz, 2H, =C*H*−), 2.2−1.2 (18H, −CH_2−). ^{13}C{^{1}H} NMR (C_6D_6): δ 132.5/133.0 (t, |$^2J_{PC}$ + $^4J_{PC}$| = 12 Hz, *o-C*), 127.5/127.6 (t, |$^3J_{PC}$ + $^5J_{PC}$| = 10 Hz, *m-C*), 128.0/128.2 (s, *p-C*), 103.9 (dt, $^1J_{RhC}$ = 5 Hz, $^2J_{PC}$ ≈ 2 Hz, ≈*C*H≈), 68.6 (m, =*C*H−), 32.3 (d, $^3J_{RhC}$ = 2 Hz, =CH*C*H$_2$−), 30.6 (t, |$^1J_{PC}$ + $^3J_{PC}$| = 24 Hz, −*C*H$_2$P), 30.0 (t, $^4J_{PC}$(cis) + $^4J_{PC}$(trans) = 6 Hz, =CHCH$_2$*C*H$_2$−), 23.3 (s, =CH(CH$_2$)$_2$*C*H$_2$−), 24.0 (t, |$^2J_{PC}$ + $^4J_{PC}$| = 8 Hz, −*C*H$_2$CH$_2$P), the *ipso-C* atoms were not detected. ^{31}P{^{1}H} NMR (C_6D_6): 38.5 (d, $^1J_{RhP}$ = 199 Hz).

X-ray Crystal Structure Analysis of [(dppb)Rh(η^3-C$_8$H$_{13}$)]·0.5C$_5$H$_{12}$ (4·0.5C$_5$H$_{12}$). X-ray data were collected on an Enraf-Nonius CAD4 diffractometer using Mo Kα radiation (λ = 0.710 69 Å). Data were corrected for Lorentz and polarization effects but not for absorption. The structure was solved by Patterson methods (SHELXS-86) and refined by full-matrix least squares against F_o^2 (SHELXL-93). Hydrogen atoms were located in the difference map. After the hydrogen atoms were included at calculated positions with fixed thermal parameters, non-hydrogen atoms were refined anisotropically. Cell parameters and other pertinent data are summarized in

Table 1. Crystallographic Data for 4·0.5C$_5$H$_{12}$

color	yellow
formula	$C_{36}H_{41}P_2Rh·0.5C_5H_{12}$
mol wt	674.6
cryst syst	monoclinic
space group	$P2_1/n$ (No. 14)
lattice param at 183 K	
a (Å)	10.252(1)
b (Å)	19.627(2)
c (Å)	18.053(1)
β (deg)	92.97(1)
vol (Å^3)	3629.4(6)
density (calcd), D_c (g cm^{-3})	1.235
no. of formula units *Z*	4
abs coeff μ(Mo Kα) (cm^{-1})	5.82
no. of collcted data	7110
no. of unique data	6733
no. of obsd data with $I \leq 2\sigma(I)$	4032
no. of variables	397
R1	0.074
wR2	0.184
residual electron density (e Å^{-3})	1.72

Table 1. Atomic coordinates, bond lengths and angles, and thermal parameters have been deposited at the Cambridge Crystallographic Data Centre. See Information for Authors, Issue No. 1.

Catalytic Hydrogenation of CO$_2$ to Formic Acid Using the *in situ* Catalyst [{(μ-H)Rh(COD)}$_4$] (1)/dppb in Acetone/NEt$_3$. **1** (12.6 mg, 14.8 μmol) and dppb (30.2 mg, 70.8 μmol) were dissolved in a mixture of 20.0 mL of acetone and 4.0 mL of NEt_3, and the mixture was stirred vigorously for 15 min. The solution was transferred to a high-pressure reactor and pressurized to 20 atm with CO_2. A total pressure of 40 atm was adjusted with H_2, and the reaction mixture was stirred with a constant rate of 750 rpm at room temperature. Samples were withdrawn after given time intervals, frozen in liquid nitrogen, and diluted with acetone-d_6 in air in order to avoid formic acid decomposition.[3b] The formic acid concentration was determined by ^{1}H NMR using NEt_3 as an internal standard.[3b] In the pre-hydrogenation experiment, the order of addition of the two gases was reversed and the solution was stirred under H_2 for 1 h before introducing CO_2.

Acknowledgment. Financial support from the Max-Planck-Society and the Fonds der Chemischen Industrie is gratefully acknowledged. We thank Degussa AG for a generous loan of $RhCl_3·3H_2O$.

Supporting Information Available: Tables giving crystal data and details of data collection, positional and thermal parameters, and bond distances and angles and an ORTEP plot of **4** (8 pages). Ordering information is given on any current masthead page.

OM950913F